

Near-IR spectroscopy of PKS1549-79: a proto-quasar revealed?

M. J. Bellamy,^{1*} C. N. Tadhunter,¹ R. Morganti,² K. A. Wills,¹ J. Holt,¹
M. D. Taylor,¹ and C. A. Watson.¹

¹*Department of Physics and Astronomy, University of Sheffield, Sheffield S3 7RH, UK*

²*Netherlands Foundation for Research in Astronomy, Postbus 2, 7990 AA Dwingeloo, The Netherlands*

To be submitted for publication in the Monthly Notices of the Royal Astronomical Society

26 November 2018

ABSTRACT

We present a near-IR spectrum of the nearby radio galaxy PKS1549-79 ($z = 0.153$). These data were taken with the aim of testing the idea that this object contains a quasar nucleus that is moderately extinguished, despite evidence that its radio jet points close to our line-of-sight. We detect broad $\text{Pa}\alpha$ emission (FWHM $1745 \pm 40 \text{ km s}^{-1}$), relatively bright continuum emission, and a continuum slope consistent with a reddened quasar spectrum ($3.1 < A_V < 7.3$), all emitted by an unresolved point source. Therefore we conclude that we have, indeed, detected a hidden quasar nucleus in PKS1549-79. Combined with previous results, these observations are consistent with the idea that PKS1549-79 is a young radio source in which the cocoon of debris left over from the triggering events has not yet been swept aside by circumnuclear outflows.

Key words: galaxies: active – galaxies: individual: PKS1549-79 – infrared: galaxies – quasars: emission lines – quasars: general

1 INTRODUCTION

In recent years, much AGN research has been conducted in the context of “unified schemes” (e.g. Barthel 1989); i.e. that differences between certain types of active galaxy can be explained by orientation effects. A great deal of AGN research is based around refining and constraining such models. However, the simplest unified models generally describe a static and unchanging situation, a steady-state regime, and this is unlikely to be realistic. As the activity evolves it is likely to affect the distribution of ISM surrounding the nucleus, potentially influencing the evolution of the host galaxy. To better understand these processes it is necessary to develop a more dynamic, evolutionary model for AGN, and to this end it is important to study sources at different evolutionary stages.

The existence of compact steep-spectrum (CSS) and gigahertz-peaked (GPS) radio sources, which are intrinsically small, illustrates the fact that there is a large range in the physical dimensions of extragalactic radio sources. The

compactness of these sources must either be due to frustration, where a dense ISM is inhibiting the expansion of the radio lobes, or to youth, in which case the radio lobes simply have not yet had time to expand. Of these two possibilities youth seems the most likely (e.g. Fanti et al. 1995). Broad forbidden lines are also much more common in these compact sources, suggesting that the cores of these sources are more unsettled (Gelderman & Whittle 1994). Moreover, Baker et al. (2002) find an anti-correlation between C IV absorption – which they show to be associated with dusty regions – and radio source dimensions; the absorption becoming less pronounced with increasing size. It is therefore becoming apparent, and perhaps expectedly so, that young radio-loud AGN suffer greater dust extinction than their more evolved counterparts, with the nucleus still surrounded by a cocoon of dust and gas.

Based on its emission line widths and kinematics, the southern radio galaxy PKS1549-79 ($z = 0.153$) appears to be just such a young source. The observed properties of this unusual object are discussed in detail in Tadhunter et al. (2001) (hereafter T2001). The flat spectrum, compactness

* E-mail: m.bellamy@sheffield.ac.uk

of the radio emission (~ 150 milliarcsec, or ~ 540 pc¹) and one-sided jet morphology of this source indicate that its radio axis is aligned close to our line-of-sight. In the standard unification model, the source would be expected to resemble a quasar at optical wavelengths, with non-stellar continuum emission and broad permitted lines. However, optical spectra of PKS1549-79 show a predominantly stellar continuum with no good evidence for broad permitted lines, but with strong and unusually broad forbidden lines (~ 1300 km s⁻¹). Amongst powerful radio galaxies such broad forbidden lines are only ever detected in sources that are intrinsically compact. The blueshift of the [O III] $\lambda\lambda 5007, 4959$ emission lines relative to low-ionisation forbidden lines and the H α 21 cm absorption line suggests that the [O III] emitting region is outflowing at 600 ± 60 km s⁻¹ (T2001, Morganti et al. 2001).

Overall, observations suggest that there is significant dust obscuration in this object even though our line-of-sight is close to the radio axis. This is entirely consistent with PKS1549-79 being a young radio source in which the obscuring material around the nucleus has not yet been swept aside (T2001). If this model is correct, near-infrared observations - being subject to only $\sim 10\%$ of the visual extinction - should show a bright, non-stellar continuum and broad permitted lines as the quasar shines through the ISM. This is the prediction we test in this paper.

2 DATA COLLECTION AND REDUCTION

The K-band infrared spectra were taken in shared risks service mode on 26 July 2002 using the IRIS2 instrument on the AAT. The Sapphire 240 grism was used with a 1 arcsec slit, oriented North-South on the sky. The seeing was reported to be 1.1 arcsec throughout the observations; analysis of stars in the 10 second exposure acquisition image is in good agreement with this (see Section 3.1). 22 exposures of 300 seconds were obtained for PKS1549-79; the galaxy was 'nodded' between two positions on the slit in an ABBA pattern with 11 exposures at each position. Four exposures of 80 seconds were taken of the A0 star HIP77712 at a similar airmass for calibration purposes.

Each set of 11 galaxy exposures was co-added in the IRAF package using median filtering to remove cosmic rays; the median 'B' image was then subtracted from the median 'A' image to remove the night sky lines. The standard star frames were combined in a similar way. The resulting galaxy and star frames were then flat-fielded using a dark-subtracted flat field taken with the same instrumental setup.

A xenon arc frame was used to make a two-dimensional wavelength calibration which was then applied to the data frames. The original spectra cover the range 20109 - 24640 Å but the useful data presented here are over the range 20500 - 23000 Å. From the night sky lines, the accuracy of the wavelength calibration was found to be ± 0.65 Å (± 9 km s⁻¹) and the systematic errors are estimated to be < 1 Å (< 14 km s⁻¹). Fits to the night sky lines show the spectral resolution to be 10.1 ± 0.4 Å; the pixel scale of 4.43

¹ We assume cosmological parameters of $H_0 = 50$ km s⁻¹ Mpc⁻¹ and $q_0 = 0$ throughout.

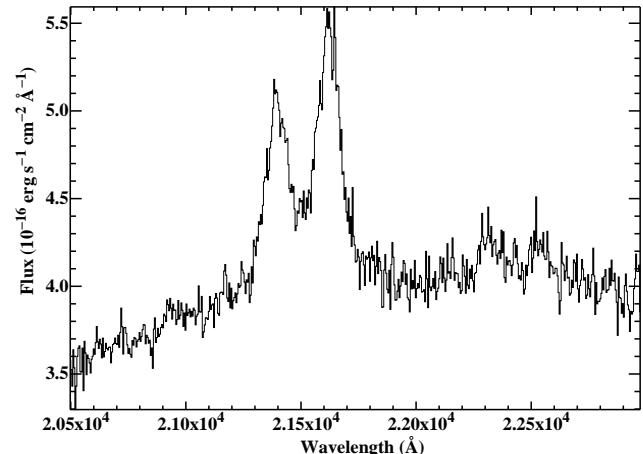


Figure 1. K-band spectrum of PKS1549-79 obtained with the IRIS2 instrument on the AAT. Doubling of the lines is caused by birefringence associated with the grism used for the observations (See Section 2).

Å pix⁻¹ is adequate to sample this. The spatial pixel scale of the acquisition image is 0.446 arcsec pix⁻¹. One-dimensional spectra were extracted from the two-dimensional frames, each from 11 pixel rows to aid accurate flux calibration.

The exposures of HIP77712 were used to flux calibrate the data, with the assumption that the intrinsic spectral energy distribution (SED) of the star is that of a perfect black body at $T = 9480$ K. The magnitude-to-flux conversion was performed with reference to Bessell, Castelli & Plez (1998).

During data reduction it became apparent that there was a problem with the IRIS2 instrument in spectroscopy mode at the time of the observations. All the spectra we had obtained, including arc calibration frames, showed a splitting of spectral features in the wavelength direction. After consulting with the AAT team we were informed that the manufacturers had mounted the Sapphire grisms at right-angles to their intended orientation and that a birefringence effect was leading to the observed doubling. The spectra we obtained are composites of the actual spectrum and a copy of this spectrum, blueshifted by around 50 pixels (~ 230 Å in the case of these data) relative to the original and at a slightly lower intensity. However, the splitting caused by the birefringence is large enough that useful kinematic information can be extracted for individual lines in the spectra. The final, reduced K-band spectrum of PKS1549-79 is shown in Fig. 1. The Starlink FIGARO and DIPSO packages were used to analyse the data.

3 RESULTS

3.1 Paschen alpha

A single Gaussian provides an adequate fit to each of the two components of the split line. The best fit to the Pa α line(s) is shown in Fig. 2, with the redder peak being at the correct wavelength. A constraint was applied that the two Gaussians should have the same width. The results of the fitting are summarised in Table 1.

The fit gives a FWHM of 126 ± 3 Å (1745 ± 40

| Parameter | Pa α | H ₂ or [Si vi] |
|--|-----------------------------------|--|
| FWHM (km s ⁻¹) | 1745 ± 40 | 1100 ± 180 |
| z | 0.15266 ± 0.00007 | 0.1525 ± 0.0002 or 0.1494 ± 0.0002 |
| Total line flux (erg cm ⁻² s ⁻¹) | $(3.16 \pm 0.08) \times 10^{-14}$ | $(3.5 \pm 1.0) \times 10^{-15}$ |
| Continuum flux (erg cm ⁻² s ⁻¹ Å ⁻¹) | $(4.0 \pm 0.1) \times 10^{-16}$ | $(4.0 \pm 0.2) \times 10^{-16}$ |
| Equivalent width (Å) | 79 ± 3 | 9 ± 3 |
| Rest-frame equivalent width (Å) | 69 ± 3 | 8 ± 3 |

Table 1. Results of the DIPSO fits to the spectral lines. The instrumental width has a negligible effect on the measured FWHMs.

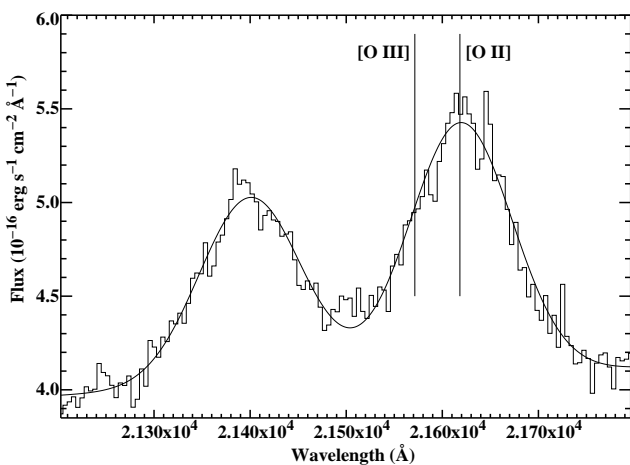


Figure 2. DIPSO fit to the Pa α line(s). Pa α wavelengths corresponding to the [O II] and [O III] redshifts (T2001) are marked for comparison.

km s⁻¹ in the rest frame). This value is consistent with the widths of permitted lines in broad line radio galaxies (BLRG) and quasars (Hill, Goodrich & DePoy 1996, Marziani et al. 2001), although it is at the lower end of the range. The relatively small broad-line widths are also consistent with the radio jet being oriented close to our line-of-sight (Wills & Browne 1986).

The redshift of the Pa α line is found to be $z = 0.15266 \pm 0.00007$. This is consistent with the [O II] redshift of $z = 0.1526 \pm 0.0002$ but inconsistent with the [O III] (outflow) redshift of $z = 0.1501 \pm 0.0002$ (T2001). This indicates that the Pa α emission originates in a broad line region (BLR) at the systemic redshift. The Pa α wavelengths corresponding to the [O II] and [O III] redshifts are marked on 2 for comparison.

The K-band continuum flux level is $\sim 4 \times$ that measured in the optical spectrum of T2001, despite the fact that the optical spectrum was obtained using a larger aperture (4.3 by 5 arcsec). This is inconsistent with the SED of an unreddened stellar population, particularly a young population, but is consistent with that of a moderately obscured quasar source shining through the intervening ISM. A power-law was fit to the continuum to aid comparisons with quasar continua (see Section 4). The spectral index of this power-law is $\alpha = 2.3 \pm 0.1$ ($F_v \propto \nu^{-\alpha}$, $F_\lambda \propto \lambda^{\alpha-2}$). This index is significantly larger than that measured for the 16 unreddened sources in the Simpson & Rawlings (2000) sample of radio-loud quasars ($-0.67 < \alpha < 1.62$), but similar to the two

reddened quasars in that sample. If the intrinsic spectrum of PKS1549-79 is quasar-like then this indicates significant reddening.

The combined flux of both Pa α components is $(3.16 \pm 0.08) \times 10^{-14}$ erg cm⁻² s⁻¹. This flux gives a rest-frame equivalent width of 69 ± 3 Å for an assumed continuum flux of $(4.0 \pm 0.1) \times 10^{-16}$ erg cm⁻² s⁻¹ Å⁻¹ in the observed frame. For comparison, the rest-frame Pa α equivalent widths measured in the low-redshift quasars 3C 273 and PDS 456 are 167 ± 16 Å and 120 ± 8 Å respectively (Hill et al. 1996, Simpson et al. 1999). Both of these quasar values are significantly larger than that measured in PKS1549-79. This could indicate the presence of a beamed, non-thermal continuum component in PKS1549-79 which would further support the theory that the radio jet is oriented towards our line-of-sight.

If there is a quasar nucleus shining through at near-IR wavelengths then the emission from the galaxy should be dominated by a central, unresolved source. To test this, the spatial intensity profile of PKS1549-79 was compared with those of four bright stars in the acquisition image. The mean FWHM of the stellar 2-D Gaussian measures 1.13 ± 0.06 arcsec in the x-direction by 1.23 ± 0.06 arcsec in the y-direction. In comparison, the profile of PKS1549-79 measures 1.13 ± 0.17 by 1.43 ± 0.15 arcsec. Therefore PKS1549-79 appears quasar-like at near-IR wavelengths.

3.2 Other features

Apart from the Pa α line, the only other feature in the spectrum is a second line visible at ~ 22550 Å, subject to the same splitting as the rest of the spectrum. As the line appears faint, the spectrum was re-binned to one-quarter resolution over this region to improve the signal to noise. The line is broad enough for this to be acceptable. The blueshifted split component is too noisy for an adequate fit to be made and so only the redmost component was fit in DIPSO. The fit is shown in Fig. 3 and the results of the fitting are given in Table 1.

The FWHM of this line is 83 ± 14 Å (1100 ± 180 km s⁻¹ in the rest frame). Correcting for the fact that only one component was fit, the total flux of the line is $(3.5 \pm 1.0) \times 10^{-15}$ erg cm⁻² s⁻¹. This corresponds to an isotropic luminosity of $(4.1 \pm 1.2) \times 10^{41}$ erg s⁻¹.

The most likely candidate for this emission is the H₂ $\nu = 1-0$ S(3) line, our identification is based on redshift arguments. The H₂ $\nu = 1-0$ line would lie at the same redshift as the Pa α line, whereas other lines imply large inflow or outflow velocities. However, [Si vi] is also a possibility since the implied outflow velocity and width are broadly consistent with the [O III] outflow parameters (T2001). The pos-

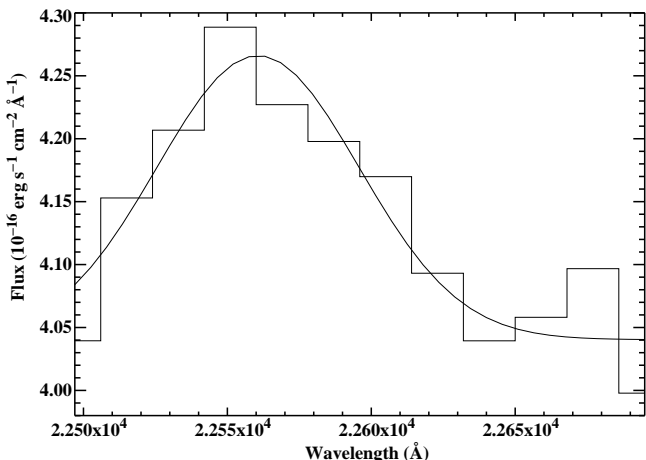


Figure 3. DIPSO fit to the $\sim 22550 \text{ \AA}$ line.

sibility that this feature is a blend of both lines cannot be discounted. However, the low S/N of the data - coupled with the uncertainties introduced by the splitting of the spectrum - means that no definite conclusions can be drawn.

If the feature is indeed $\text{H}_2 \nu = 1-0 \text{ S}(3)$, then PKS1549-79 is one of the most luminous molecular hydrogen emitters in the local universe, surpassing the H_2 luminosity of Cygnus A by almost an order of magnitude (Ward et al. 1991, Thornton, Stockton & Ridgway 1999).

Unfortunately no other molecular hydrogen lines are visible in the spectrum with which to compare this result. This is to be expected however, as the $\text{H}_2 \nu = 1-0 \text{ S}(3)/[\text{Si VI}]$ feature is only weakly detected and the only molecular line expected to be comparable in luminosity ($\text{H}_2 \nu = 1-0 \text{ S}(1)$) is redshifted out of the useful range of our data.

4 DISCUSSION

Our observations provide clear evidence that emission from the central regions of PKS1549-79 is significantly affected by dust obscuration. In this section we attempt to estimate the degree of reddening² and correct for it in order to obtain a more realistic estimate of the intrinsic $\text{Pa}\alpha$ luminosity. For comparison, T2001 derive a visual extinction in the range $0.23 < \text{A}_V < 18$ mag, based on HI 21 cm absorption characteristics.

Firstly, we try to determine the reddening directly from Balmer line ratios, these being relatively insensitive to variations in the physical conditions of the emitting medium. With reference to Tadhunter et al. (1993), the $\text{Pa}\alpha/\text{H}\beta$ line ratio is found to be 25 ± 1 . Assuming Case B recombination, a temperature of 10,000K and an electron density of $10^4 \text{ electrons cm}^{-3}$, this line ratio gives an $E_{B-V} = 1.29 \pm 0.01$ (Seaton 1979, Osterbrock 1989), corresponding to a visual extinction of $\text{A}_V = 4.00 \pm 0.13$ mag ($\text{A}_V = R \times E_{B-V}$, assuming $R = 3.1 \pm 0.1$). However, there is a great deal of uncertainty associated with this value because the $\text{H}\beta$ emission is likely to be dominated by a narrow line region (NLR)

² We assume the standard interstellar extinction law of Whitford (1958).

component. The BLR emission from within the obscuring region may then contribute only a fraction, if any, of the total $\text{H}\beta$ flux, and therefore the derived extinction is likely to be an underestimate. Recently obtained high-resolution spectra of PKS1549-79 include $\text{H}\alpha$ emission: however, the $\text{H}\alpha$ line is contaminated with bright N II recombination lines and an atmospheric absorption line. These features will significantly reduce the accuracy of line fittings to the $\text{H}\alpha$ line and for this reason the line has not been used in this analysis.

Another approach is to fit a power-law to the near-IR continuum and then calculate the de-reddening necessary to make the slope consistent with a quasar spectrum. As stated in Section 3.1, the spectral index of the power-law fit to our data is $\alpha = 2.3 \pm 0.1$. Typical unreddened quasar spectral indices lie in the range $-0.67 < \alpha < 1.62$ and average $\bar{\alpha} = 0.90$ (Simpson & Rawlings 2000). Clearly the spectrum for PKS1549-79 is considerably redder than even the upper limit. De-reddening of the spectrum to match the quasar range of values requires a visual extinction in the range $1.8 < \text{A}_V < 8.0$ with $\text{A}_V = 3.8$ for the average case. The full de-reddening results are given in Table 2. If the spectrum is contaminated by a beamed, non-thermal component then the intrinsic continuum shape may not resemble a quasar; in the extreme case it may more closely resemble a BL Lac. The 6 BL Lacs in the Massaro et al. (1995) sample show a tighter range of spectral indices ($0.86 < \alpha < 1.19$) with an average that is redder than that of the quasar sample: this may imply a smaller degree of reddening. However, as the full range of BL Lac spectral indices lies within the broader range of quasar spectral indices, this result has no significant effect on our analysis.

To investigate the contribution such reddened power-law continua would make at optical wavelengths, curves were generated for the derived power-laws and then re-reddened by the corresponding amount. Fig. 4 shows the results of this for the maximum, average and minimum extinctions/power-laws derived above. Certainly, the minimum reddening case is ruled out on the basis that the quasar alone would contribute more flux at $> 6000 \text{ \AA}$ than is detected (T2001). The average extinction, corresponding closely with that derived from the $\text{Pa}\alpha/\text{H}\beta$ ratio, would also be contributing around half the observed flux in this region and also with a marked slope that one would expect to detect superimposed on the starlight: modelling shows no evidence for a power-law component in this region (Tadhunter et al. 2002). This implies that the actual reddening is closer to the upper limit than to the average, regardless of whether the intrinsic continuum slope more closely resembles a quasar or BL Lac. It seems safe to conclude that the total visual extinction lies in the range $3.8 < \text{A}_V < 8.0$ mag. This corresponds to an intrinsic extinction in the host galaxy of $3.1 < \text{A}_V < 7.3$, having corrected for the Galactic extinction of $\text{A}_V = 0.68$ (Schlegel, Finkbeiner & Davis 1998).

The de-reddened $\text{Pa}\alpha$ fluxes for the three cases are given in Table 2, along with the corresponding isotropic luminosities. Comparison with similarly derived luminosities for a sample of quasars and BLRGs (Rudy & Tokunaga 1982, Hill et al. 1996 and Simpson et al. 1999) shows that the luminosity corresponding to the average reddening ($(59.0 \pm 1.5) \times 10^{41} \text{ erg s}^{-1}$) is more than an order of magnitude less than that measured in the low- z quasars, and at the upper

| Reddening Degree → | Minimum | Average | Maximum |
|--|-----------------|-----------------|-----------------|
| Spectral Index α | 1.62 | 0.90 | -0.67 |
| E_{B-V} | 0.60 | 1.23 | 2.62 |
| A_V (total) | 1.8 | 3.8 | 8.0 |
| A_V (intrinsic) ^a | 1.2 | 3.1 | 7.3 |
| $\text{Pa}\alpha$ Flux ($10^{-14} \text{ erg s}^{-1} \text{ \AA}^{-1}$) | 3.95 ± 0.10 | 5.02 ± 0.13 | 8.50 ± 0.22 |
| $\text{Pa}\alpha$ Luminosity ^b ($10^{41} \text{ erg s}^{-1}$) | 46.4 ± 1.2 | 59.0 ± 1.5 | 99.8 ± 2.5 |

Table 2. Resulting $\text{Pa}\alpha$ emission parameters corresponding to the different degrees of reddening as discussed in the text.

^a Assuming Galactic extinction $A_V = 0.68$ (Schlegel et al. 1998).

^b Calculated assuming isotropic emission.

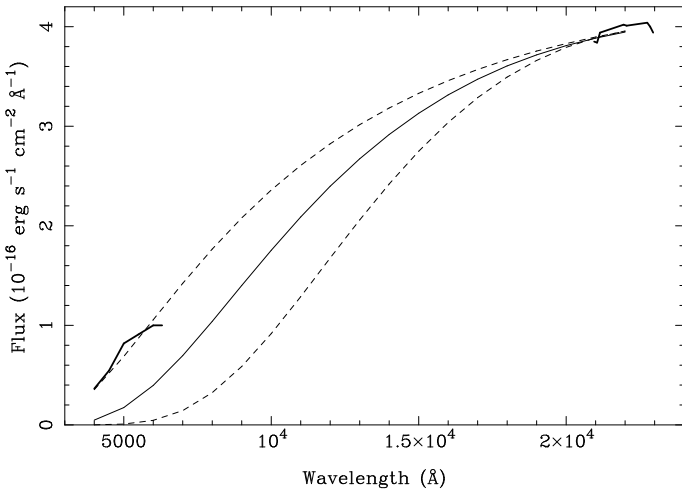


Figure 4. Reddened power-laws generated for the parameters given in Table 2. The average case is shown by the solid line, the minimum case by the upper broken line and the maximum case by the lower broken line. The thick solid lines represent the optical continuum data from T2001 and the near-IR data from this paper. The data are plotted at the observed wavelengths and the model shifted into this frame to match.

end of the range measured in the BLRGs. These results are consistent with PKS1549-79 being a low-luminosity quasar.

5 CONCLUSIONS AND FURTHER WORK

The detection of a broad $\text{Pa}\alpha$ line and a bright, reddened infrared continuum indicates that we have, indeed, uncovered an obscured BLR and quasar nucleus in PKS1549-79. The calculated intrinsic luminosity and equivalent width of the $\text{Pa}\alpha$ emission, and the star-like profile of the near-IR nucleus, further support this conclusion. Although such findings are not unprecedented (Djorgovsky et al. 1991, Hill et al. 1996), PKS1549-79 is a special case since the observed radio properties lead us to believe that the AGN is viewed from a direction close to that of the radio axis and should therefore exhibit the optical/infrared properties of radio loud quasars; i.e. no significant obscuration of the BLR and nucleus. The fact that significant obscuration is seen suggests that PKS1549-79 is a fundamentally different type of object that does not fit neatly into standard unified schemes.

It is our suggestion that PKS1549-79 is an AGN in the

early stages of evolution, a proto-quasar. The high obscuration is a transitory phase that will pass as the gas and dust is dissipated or blown out of the ionisation cones by the circumnuclear outflows detected at optical wavelengths (T2001). These infrared data support this model and tie in well with expectations.

Since a key assumption of the model is that the radio jet is oriented towards us, it is important to validate this assumption. The fact that the $\text{Pa}\alpha$ equivalent width is noticeably smaller than that for a typical quasar is consistent with the presence of a beamed continuum component and may therefore support this assumption. However, this is not sufficient evidence in itself. Multi-epoch VLBI imaging of the radio emission could provide incontrovertible evidence that the radio axis is oriented towards us by revealing superluminal motion in the jet.

ACKNOWLEDGEMENTS

We thank Chris Tinney and Stuart Ryder of the Anglo-Australian Telescope for taking the observations and for their assistance during data reduction. We also thank the referee for his useful comments and corrections. MJB and JH are supported by PPARC studentships; MDT is supported by a University of Sheffield studentship; KAW is supported by a Dorothy Hodgkin Royal Society Fellowship.. We acknowledge the data analysis facilities at Sheffield provided by the Starlink Project, which is run by CCLRC on behalf of PPARC. The Anglo-Australian Telescope is operated at Siding Springs by the AAO.

REFERENCES

- Baker J. C., Hunstead R. W., Athreya R. M., Barthel P. D., de Silva E., Lehnert M. D., Saunders R. D. E., 2002, ApJ, 568, 592
- Barthel P. D., 1989, ApJ, 336, 606
- Bessell M. S., Castelli F., Plez B., 1998, A&A, 333, 231
- Djorgovsky S., Weir N., Matthews K., Graham J. R., 1991, ApJ, 372, L67
- Fanti C., Fanti R., Dallacasa D., Schilizzi R. T., Spencer R., Stanghellini C., 1995, A&A, 302, 317
- Gelderman R., Whittle M., 1994, ApJS, 91, 491
- Hill G. J., Goodrich R. W., DePoy D. L., 1996, ApJ, 462, 163
- Marziani P., Sulentic J. W., Zwitter T., Dultzin-Hacyan D., Calvani M., 2001, ApJ, 558, 553

Massaro E., Nesci R., Perola G. C., Lorenzetti D., Spinoglio L., 1995, A&A, 299, 339

Morganti R., Oosterloo T. A., Tadhunter C. N., van Moorsel G., Killeen N., Wills K. A., 2001, MNRAS, 323, 331

Osterbrock D. E., 1989, *Astrophysics of Gaseous Nebulae and Active Galactic Nuclei*. University Science Books, California

Rudy R. J., Tokunaga A. T., 1982, ApJ, 256, L1

Schlegel D. J., Finkbeiner D. P., Davis M., 1998, ApJ, 500, 525

Seaton M. J., 1979, MNRAS, 187, 73P

Simpson C., Rawlings S., 2000, MNRAS, 317, 1023

Simpson C., Ward M., O'Brien P., Reeves J., 1999, MNRAS, 303, L23

Tadhunter C., Dickson R., Morganti R., Robinson T., Wills K., Villar-Martin M., Hughes M., 2002, MNRAS, 330, 977

Tadhunter C. N., Morganti R., di Serego Alighieri S., Fosbury R. A. E., Danziger I. J., 1993, MNRAS, 263, 999

Tadhunter C. N., Wills K., Morganti R., Oosterloo T., Dickson R., 2001, MNRAS, 327, 227

Thornton R. J., Stockton A., Ridgway S., 1999, AJ, 118, 1461

Ward M. J., Blanco P. R., Wilson A. S., Nishida M., 1991, AJ, 382, 115

Whitford A. E., 1958, AJ, 63, 201

Wills B. J., Browne I. W. A., 1986, ApJ, 302, 56